CrossMark

Oxidation Behavior of Al$_2$O$_3$ Coating on Ti-25Al-12.5Nb Alloy

J. Małecka

The oxidation behavior of Al$_2$O$_3$ coating deposited on Ti-25Al-12.5Nb alloy by sol-gel method was investigated at 700 and 800 °C under isothermal oxidation conditions in air. At both temperatures, the coated samples exhibited reduced mass gain compared to uncoated alloy; at 700 °C rather insignificant differences were observed; however, at the temperature of 800 °C, the deposited coating strongly limits the mass gain of the test material. As a consequence of the isothermal oxidation a scale forms containing mainly TiO$_2$ on the alloy surface of the uncoated alloy, while during the oxidation of the coated alloy the surface coating of Al$_2$O$_3$ dissociated and the initially compact Al$_2$O$_3$ coating dissolved and its place was taken by a porous scale. These coated samples displayed good resistance to oxidation in set conditions and no zones of dissolved oxygen and nitrogen were recorded. No spallation of the coated samples was observed.

1. Introduction

Titanium aluminide alloys represent an important class of materials, providing a unique set of physical and mechanical properties that can bring substantial advantages in future aircraft engines (Ref 1). Low density and good strength at high temperatures or creep resistance cause the alloys to have versatile applications (Ref 2-4). The two intermetallic compounds, α_2-Ti$_3$Al and γ-TiAl, are the most attractive materials, which create a commercial basis in aerospace, aircraft, and automobile applications (Ref 5). However in titanium aluminide alloys, orthorhombic Ti$_2$AlNb alloys exhibit better creep resistance as well as higher ductility and fracture toughness than α_2-Ti$_3$Al- and γ-TiAl-based alloys (Ref 6), but its poor oxidation resistance at high temperatures limits their application (Ref 7).

Many reports describe the oxidation behavior of γ-TiAl alloys, but little work has been done about the improvements of oxidation resistance of Ti$_2$AlNb alloys. On the other hand, further investigation and improvement of the oxidation resistance are necessary and are also a challenge for developing orthorhombic Ti$_2$AlNb alloys. An alloy's heat resistance depends primarily on the protective properties of the scale that forms in the course of oxidation. However, in high temperature, the formed scale is insufficient for the protection of the substrate material, resulting in its complete or partial destruction.

One way of improving oxidation resistance is the application of appropriate protective coatings. The extension of its lifetime can be achieved by coating its surface with a special layer of protective nature. The coating and the substrate protected by it must be treated as an integral entity under working conditions. Therefore, the selection of the coating material should incorporate a number of the specific requirements for the metal substrate-coating system. The coating should be stable during its use and have many properties consistent with the properties of the substrate material. Therefore, the rate of diffusion exchange between the two elements of the system must be small compared to the time of use. The protective layer and the substrate must have similar coefficients of thermal expansion to prevent cracking and peeling of the coating during temperature changes. The protective coating is also required to feature the ability for self-healing of microcracks or microdefects occurring during its use. Finally, a good coating should be relatively easy to obtain. In most cases, a good protection of the material is desired for a long time, but in some cases operating time of the element is limited by other parameters, as it is for example in rocket engines.

Recent investigation on the oxidation behavior of Ti$_2$AlNb was carried out in terms of protective coatings. Braun and Layens reported the oxidation protection of TiAlCr and TiAlCrYN coatings (Ref 8) which were successful in the protection of the substrate alloy at 750 °C. S. G. Warrier studied the γ-TiAl coating (Ref 9) which showed excellent oxidation resistance during thermal cycling conditions. Lingyan Kong et al. investigated the oxidation resistance of TiAl$_3$-Al composite coating on orthorhombic Ti$_2$AlNb alloy (Ref 10). The results showed good performance in protecting orthorhombic alloy against high-temperature oxidation at 950 °C.

Coatings and surface modification of materials are of considerable interest because they can be used to tune their physical, chemical, and even biological properties (Ref 11-13). A good example is sol-gel process which allows to obtain, in a relatively low-temperature multi-component material with properties controlled at the molecular level (Ref 14). Compared to conventional thin film processes, this technique allows for better control of the chemical composition and microstructure of the coating, preparation of homogeneous films, reduction of the densification temperature, and last but not least, simpler equipment and lower cost (Ref 15).

J. Małecka, Opole University of Technology, S. Mikołajczyka 5 Street, 45-271 Opole, Poland. Contact e-mail: j.malecka@po.opole.pl.

The research studies presented in this paper use the sol-gel method for applying layers which results in producing Al_2O_3 layers with increased efficiency.

2. Experimental Procedures

The tests were performed on O-Ti_2AlNb-based Ti-25Al-12.5Nb (at.%) alloy with a content of β-stabilizing elements: Mo (6.01 at.%) and V (0.48 at.%). Oxidation tests were carried out on rectangular coupons of $20 \times 15 \times 2$ mm. The samples were polished with 800 grade paper and subsequently degreased in acetone. The Al_2O_3 layer was obtained by sol-gel method (Ref 14, 16). The technology of producing oxide layers synthesized by the sol-gel method applied by means of dip-coating (layer deposited from liquid phase) was used to deposit Al_2O_3 layer. The stabilization of Al_2O_3 surface was carried out by means of thermal method (temperature 800 °C) while the dip/resurface rate was 34 mm/min.

Isothermal oxidation experiments were performed in static air atmosphere at the temperature 700 and 800 °C. The samples with Al_2O_3 coating of 3 μm obtained were heated up with the furnace, during 50, 100, 300, and 500 hours, and subsequently cooled down to the room temperature. After the specific annealing times (50, 100, 300, and 500 hours, respectively), each time one of the samples was removed from the furnace and after cooling, it was weighed using a precise analytical scales in order to determine the kinetics of the mass change resulting from the forming corrosion layers on the surface of the samples. Such a procedure was assumed for the whole research cycle. The computer-aided acquisition system was used to verify the actual test temperature. Mass changes due to oxidation processes were controlled by precision scale with accuracy of 10^{-4} g. Trials were repeated three times and the presented test results were averaged. For comparison, the reference alloys were samples of the alloy without the coating.

After the test was finished, surfaces and cross section of the oxidized specimen were characterized. They were studied by scanning electron microscopy (SEM) and were also subjected to energy-dispersive x-ray microanalysis. Investigations of the material structure and chemical constitution in the micro-areas of the specimens were performed using a JEOL JSM-35 microscope equipped with a WDS analyser and Philips XL20 microscope equipped with an EDS analyser.

3. Test Result and Analysis

The oxidation kinetics of the coated and uncoated O-Ti_2AlNb alloy is presented in Fig. 1 (continuous curves for initial state alloy and dashed curves for the alloy coated with Al_2O_3).

During the oxidation at the temperature of 700 °C, the difference between the coated and uncoated alloy is practically insignificant while at the temperature of 800 °C significant differences were observed in favor of the alloy coated with Al_2O_3. For the uncoated alloy, at the temperature of 700 °C, the thermogravimetric curve was characterized by a big mass gain in the initial period lasting about 100 hours, and a subsequent noticeable slow-down. As can be seen after 500 hours, the mass gain of the alloy is far smaller than that at 800 °C. Up to 500 h,

the mass change did not exceed 0.2 mg/cm^2. At the temperature of 800 °C, the thermogravimetric curve was characterized by an exceptionally big mass gain during the oxidation test. The mass change progressively increases, reaching about 1.1 mg/cm^2 after 500 h for the uncoated alloy, and 0.8 mg/cm^2 for the coated alloy. For Al_2O_3-coated alloy oxidized at 700 °C rather insignificant differences were observed. Mass gains in this case are about 0.02 mg/cm^2 less compared to the bare alloy, and in consequence after 500 h of oxidation, the mass gain reaches a comparable level. But, at 800 °C, the uncoated alloy shows approximately linear, not parabolic, oxidation kinetics. As observed at 800 °C, the alloy shows normalized weight gain, but the kinetics are significantly different. After the first period of a protective behavior, the alloy shows approximately linear behavior after 100 h, then after 300 h the oxidation rate accelerates. During the oxidation at the temperature of 800 °C, the deposited coating strongly limits the mass gain of the test material, after both 50, 100, 300, and 500 h and the thermogravimetric curve is characterized by a parabolic course of reaction.

The oxide scales were brittle and showed local cracking after cooling, but there was no evidence of spallation during the experiments. The scale forming on the surface of samples was tightly attached to the substrate and did not chip either immediately after the test or later. Despite the fact that during the tests and immediately after their completion the scale formed on the coated and uncoated alloy showed good adhesion to metallic substrate, under the influence of dynamic strain loads, products near the fracture line of the uncoated alloy partially chipped already after the oxidation at the temperature of 700 °C (Fig. 2). Such chipping was not observed for coated specimens.

The course of oxidation based on going research with the determination of weight gains of the oxidized alloy Ti-25Al-12.5Nb can be described by the relevant kinetic laws associating the thickness of the product with the temperature and oxidation time. At the temperature of 800 °C through almost entire the time range the oxidation takes place similarly to linear correlation, only after some time for the coated alloy (after 300 h of oxidation) there is an intermediate region between the linear and parabolic. Through the remaining temperature range (700 °C), a sub-range can be distinguished with a course similar to linear or intermediate (up to 50 h of oxidation); only with the elongation of the oxidation time a correlation close to parabolic is observed. The obtained reflection of changes in the amount of oxygen absorbed over time by the tested material leads to the conclusion that the reaction rate varies with the increase of oxidation time. In the initial stage of oxidation, the variation from the parabolic course towards the linear relationship is observed and subsequently it returns to parabolic correlation. Mostly, the oxidation process is subject to general power law when the thickness of the reaction products layer is directly proportional to the mass of the oxidant bound per unit area. Assigning the physical meaning to the activation energy, namely defining it as the diffusion activation energy in the process of oxidation is possible when parabolic course of the process is accompanied by the formation of a compact single-phase product. The oxidation of the alloy Ti-25Al-12.5Nb leads to the formation of multi-phase layers of not only different phase compositions, but also morphology. The tested alloy undergoes bidirectional diffusion, whereby a portion of the oxygen and nitrogen are not only "consumed" for the formation of the product, but also for
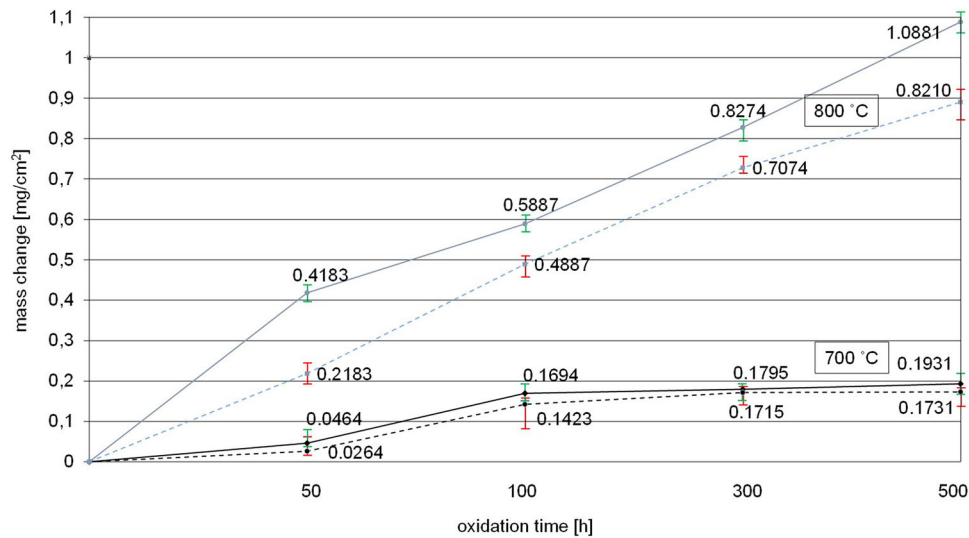
Fig. 1 The mass change of Ti-25Al-12.5Nb alloy oxidized isothermally at 700 and 800 °C (continuous curves for initial state alloy and dashed curves for the alloy coated with Al_2O_3)
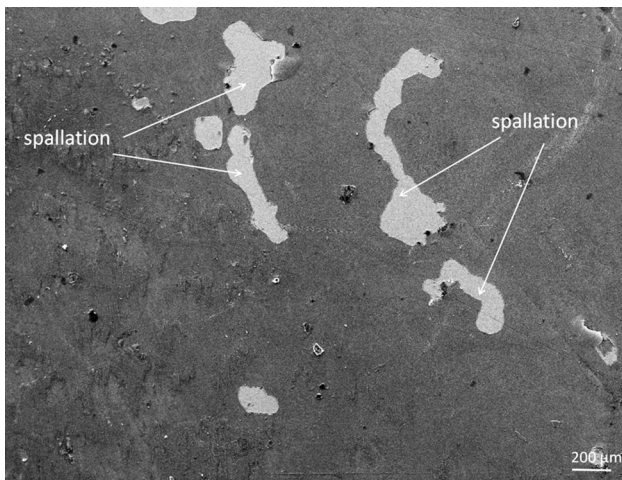

Fig. 2 Fragmentary chipping of products resulting from a fracture of a sample

the formation of the interstitial solid solution in the metallic substrate. In addition, the layer thickness is also affected by the number and arrangement of the pores (Fig. 5, 8), and the mass gain is also affected whether more Al or Ti is bound. Thus, generally, it can be stated that the layer thickness in the present case is not proportional to the mass of the oxidant, so the oxidation course is so different from the parabolic.

3.1 Cross Section and Surface Analysis of Uncoated Alloy

After oxidation in static air, the analyzed uncoated alloy is characterized by the formation of scale as the reaction product and the formation of the diffusion area of interstitial elements in the metallic substrate. Oxide layers forming during annealing consist of a few characteristic sublayers. The chemical analysis (at.%) of each layers is presented in Table 1.

X-ray diffractometry image of the oxidized uncoated O-Ti_2AlNb alloy, in the form observable in Fig. 3, showed TiO_2 (rutile) and Al_2O_3 (in lesser degree), which can be observed in

other analyses of orthorhombic alloys (Ref 17, 18). The surface characterized by quite an irregular structure in the form of particular efflorescences (Fig. 4), loosely covering the next sublayer. The middle sublayer forms a band running parallel to the oxidized surface and characterized by a graphite-gray contrast in BSE, which is, however, heterogeneous (Fig. 5). This sublayer shows the dominance of Al with a much lower share of Ti. Probably, this band has a lot of Al_2O_3 but little TiO_2. Since these oxides occur separately, it results in the heterogeneity of the contrast and strong diversification of the composition in nano-areas. Aluminum cations which diffuse out-core (slower than Ti) form Al_2O_3 with the oxygen. A protective layer will be formed from the reaction products only when they exclusively contain Al_2O_3. The formed layer of Al_2O_3 is heterogeneous and not compact. Rutile TiO_2 is also present in its composition, however, in lower quantities. The presence of even a little quantity of TiO_2 in the sublayer rich in Al_2O_3 allows bidirectional diffusion and, as a result, the growth of the product on the outer surface as well as on the product-metallic substrate interface. The inner layer contains locally higher quantities of TiO_2. Moreover, it contains oxides of alloying elements included in the composition of the analyzed alloy. Catenary microbands can be distinguished in this sublayer enriched in niobium, arranging parallel to the surface of the oxidized specimen. As it was determined, however, the remaining alloying elements add to changing the mass transfer course through the product layer. Linear distribution of Ti, Al, Nb elements plotted for the scale and the substrate is shown in Fig. 6. The distribution is consistent with the previously presented concentration of particular elements in the oxide layers. In the outer layer, the dominance of Ti, growth of Al in the middle layer, and the presence of Nb-rich region near to metallic substrate were found.

The scale formed on the uncoated alloy showed the concentration of fine pores and a layered structure made of alternate layers. This is due to the fact that Ti has been selectively oxidized to TiO_2, under which the elements Nb and Al were relatively enriched. Then the oxygen diffusing through a layer rich in TiO_2 reacted with Nb and Al, which allowed for the formation of a layer most likely enriched in $AlNbO_4$. Under the layer rich in $AlNbO_4$, Ti is enriched again. Therefore, a

Table 1 WDS-Analysis (at.%) of Locations Layers on Fig. 5

Element	N	O	Al	Nb	Ti	Mo	V
Outer layer	…	56.49	11.84	4.85	23.82	…	…
Middle layer	…	55.62	37.27	0.72	5.83	0.56	…
Inner layer	…	54.98	21.00	1.98	20.87	0.80	0.37
Interface	16.60	19.00	20.82	8.91	33.35	1.20	0.12
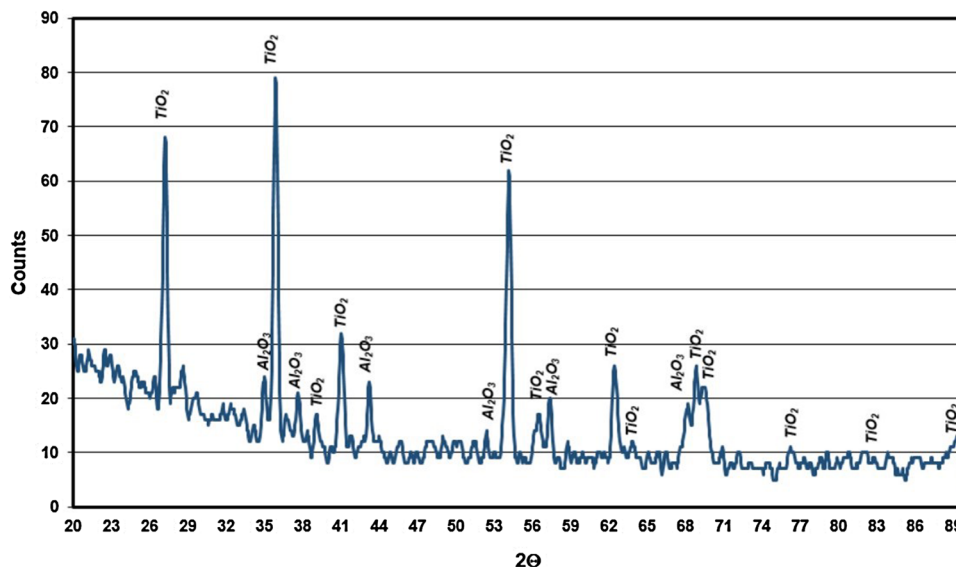
Fig. 3   XRD microanalysis result of surface uncoated alloy after isothermal oxidation

multilayer scale is formed consisting of alternating layers rich in TiO_2 and $AlNbO_4$. Similar to reports in the literature (Ref 18), oxygen and nitrogen were present in the interface between the oxide scale and the metallic substrate, and subsurface embrittlement caused by the formation of the nitride layer and the penetration of air / nitrogen was evident (microvoids).

3.2 Cross Section and Surface Analysis of Coated Alloy

In the case of Ti-25Al-12.5Nb coated with Al_2O_3, it can be said that the coating plays an important role in protecting the base material against further oxidation, which results in smaller mass gains, in particular at 800 °C (Fig. 1). During the exposure to high-temperature reaction, products are formed on the surface of the coating layer, because diffusion exchange takes place between the components of the alloy and the protective layer. This phenomenon is advantageous because it leads to the increased adhesion of the coating to the substrate. In addition, this leads to significant changes in the composition of material and protective layer near the coating-substrate interface. It was observed that the deposited layer inhibits the course of the oxidation of the tested alloy.

The thermal expansion coefficient of the materials used has a significant impact here. Thus, the difference in coefficients of thermal expansion of the substrate and the deposited coating is negligible. The coefficient of thermal expansion of Ti_2AlNb alloy is 8.8×10^{-6} K^{-1} (Ref 19) and of the Al_2O_3 coatings is 8.3×10^{-6} K^{-1} (Ref 20). For this reason, the top layer consisting of Al_2O_3 may be a promising material as oxidation-resistant alloy coating based on the orthorhombic phase.
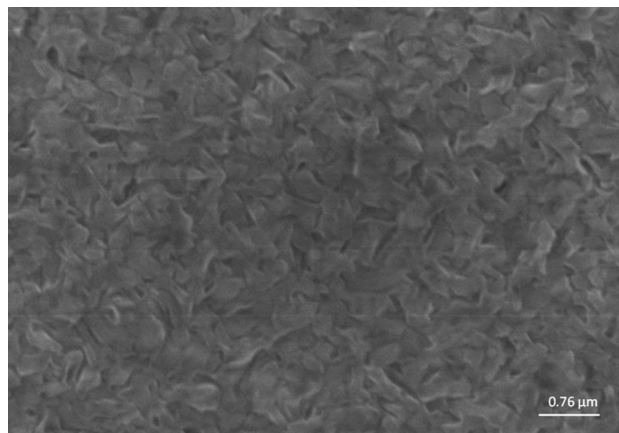
Fig. 4   Surface of uncoated alloy after isothermal oxidation

In Fig. 7, a view of the surface of the alloy coated with Al_2O_3 oxidized in the air is presented, while Fig. 8 shows a cross section through the substrate and the formed oxide layer (chemical compositions of the different sublayers are shown in Table 2). However, the linear distribution is presented in Fig. 9. The porous outer layer is visible over the entire surface of the coated alloy.

During the oxidation of the alloy with the coating, probably the dissociation of Al_2O_3 coating occurs, and the oxygen diffusing to the substrate from the coating reacts with Ti and forms TiO compounds during the oxidation process. Linear
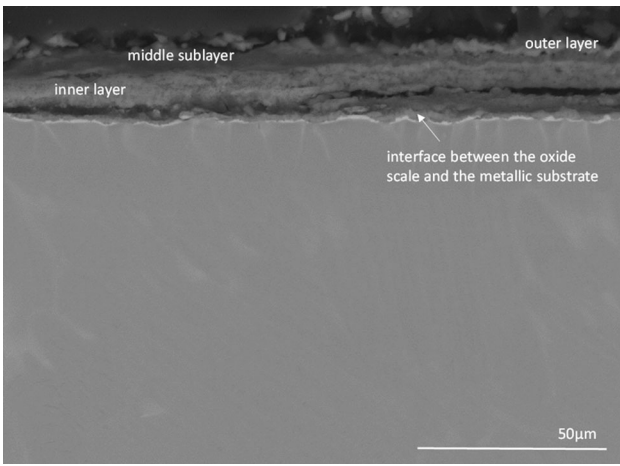
Fig. 5 Cross section of products and metallic sublayer of uncoated alloy after isothermal oxidation
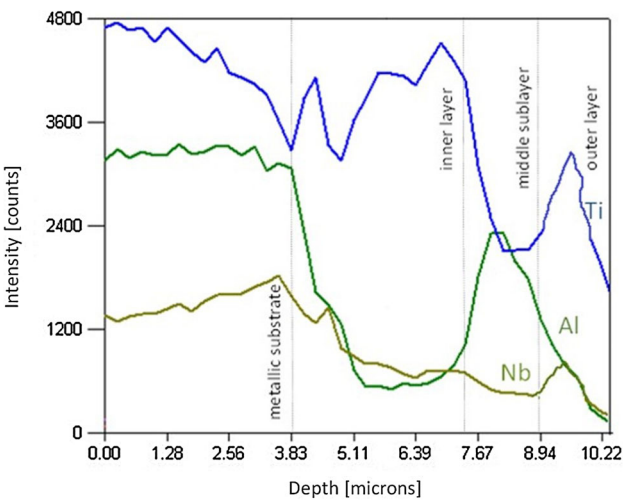

Fig. 6 Linear distribution of Ti, Al, and Nb elements (on cross section of products and metallic sublayer of uncoated alloy after isothermal oxidation)
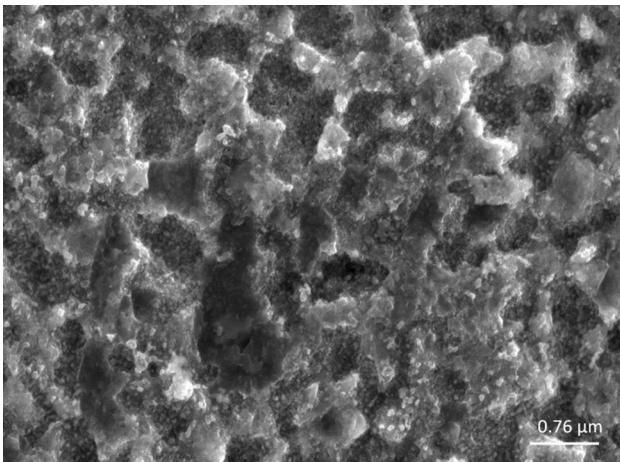

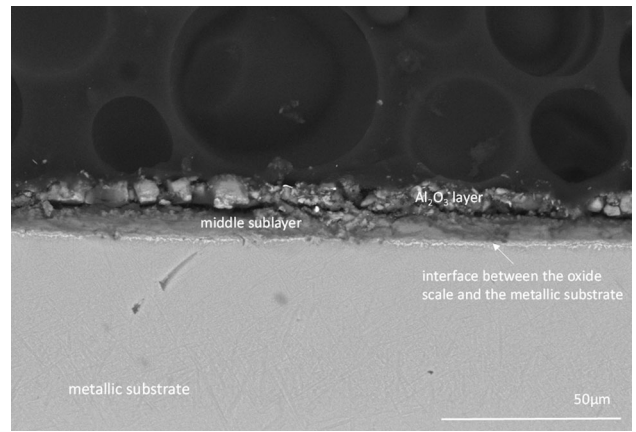**Fig. 7** Surface of coated alloy after isothermal oxidation

Fig. 8 Cross section of products and metallic sublayer of coated alloy after isothermal oxidation

distribution of elements (Fig. 9) illustrates that oxygen from the Al_2O_3 coating diffuses directly into the alloy to the depth below the deposited coating. Niobium originating from the substrate of the alloy does not react with Al_2O_3 layer, which is confirmed by tests carried out by Mader and Rühler (Ref 21) who established that no reaction layer is formed between the Nb and Al_2O_3 in the high-temperature oxidation. Al_2O_3 compound reacts with Ti because of the high solubility of oxygen in titanium and occurring diffusion of oxygen to the metallic substrate.

Al_2O_3 compound reacts with Ti because of the high solubility of oxygen in titanium. The mechanism of the reaction that occurs between the alloy Ti-25Al-12.5Nb and the Al_2O_3 coating results from the decomposition of

$$Al_2O_3 = 2(Al) + 3(O),$$
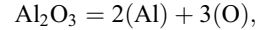
where (Al) is Al^{3+} and (O) is O^{2-}, and occurring diffusion of oxygen to the metallic substrate. This reaction results in

$$(O) + (Ti) = TiO,$$
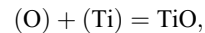
where (O) is O^{2-} and Ti is Ti^{2+}.

The question is why a scale of such type is formed on the surface? The reason behind it is that the thermodynamical stability of TiO is similar to Al_2O_3 (Fig. 10) and this limits the selective oxidation of Al into Al_2O_3, so the metal based on titanium also undergoes oxidation (Ref 22). Moreover, due to a strong disorder of the crystal lattice, TiO and other titanium oxides (most frequently TiO_2 as this oxide is quickly oxidized to dioxide) grow fast and do not form the protective oxide layer. It must be emphasized that the stability of TiO and Al_2O_3 depends on the content of respective elements in the alloy. The research by Eckert'a i Hilpert'a (Ref 23) showed that a stable Al_2O_3 oxide is formed with the content of 54 at.%. Al, whereas below this concentration TiO is a more stable oxide. Rahmel, Spencer oraz Luthra (Ref 24, 25) prove that the scale made of Al_2O_3 can be formed if the concentration of aluminum in the alloy exceeds 55 at.% (Fig. 11), and below that concentration the activity of aluminum is lower than titanium and the oxide which shows better thermodynamical stability is TiO in this case. Other calculations based on analyses of the activity of Al and Ti in Ti-Al-O show that TiO is more stable than Al_2O_3 (Ref 26, 27), but the exact opposite

Table 2 WDS-Analysis (at.%) of Locations Layers on Fig. 8

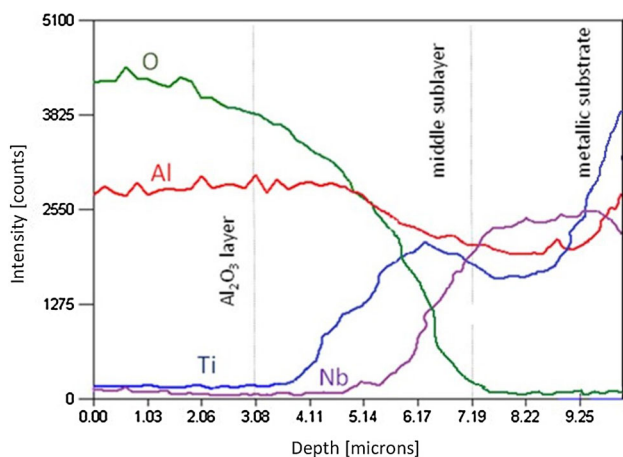| Element	N	O	Al	Nb	Ti	Mo	V
Al_2O_3 layer	…	48.12	44.61	…	7.27	…	…
Middle layer	…	25.92	38.21	2.13	33.74	…	…
Interface	…	23.11	26.94	17.32	29.98	2.31	0.34

Fig. 9 Linear distribution of Ti, Al, Nb, and O elements (on cross section of products and metallic sublayer of coated alloy after isothermal oxidation)

Fig. 10 Dissociation pressures of selected oxides vs. temperature. Curves for TiO and Al_2O_3 are close together [34]

phenomenon was observed in experimental studies, where the Al_2O_3 was undeniably more stable than TiO. What's interesting, it did not only affected areas of γ and $\gamma + \alpha_2$ present in titanium aluminides, but also in cases where the aluminum content was in the range of 1-25 at.% (Fig. 12) (Ref 28-31). Among the reasons for the discrepancies between the thermodynamic calculations, and the experimentally determined phase diagram of Al-Ti-O, the different solubilities of oxygen in the Ti-Al phases are often listed as the key reason. They were omitted in the early thermodynamic calculations while they can have significant importance for the formation of respective oxide phases (Ref 30, 32). Thermodynamic modeling shows that the calculation of the phase diagram Ti-Al-O may better reflect experimental studies if the solubility of oxygen is taken into account (Ref 33).

Thermodynamic data such as the standard enthalpy of formation of a compound or dissociation pressure allow predicting oxidation products, but they do not provide information about the speed of the reaction. In many cases, the formation of thermodynamically desirable phases may be so slow that less stable oxides are formed in the first place. Moreover, it should be added that if the activity of a single element in the alloy is less then unity compounds can be formed or there is a total or limited miscibility in the solid state. Therefore, in many cases, assumptions for two-element alloys cannot be used for more complex alloys. This results in the demand for phase diagrams of ternary systems, or even multi-element systems, and in particular for various gas mixtures, however, their availability is very limited.

During the oxidation of this alloy, it is noted that also in this case a light layer is formed (interface between the oxide scale and the metallic substrate), which was identified as the
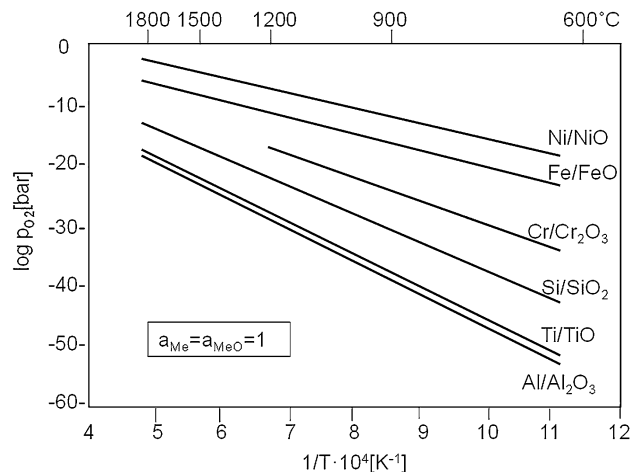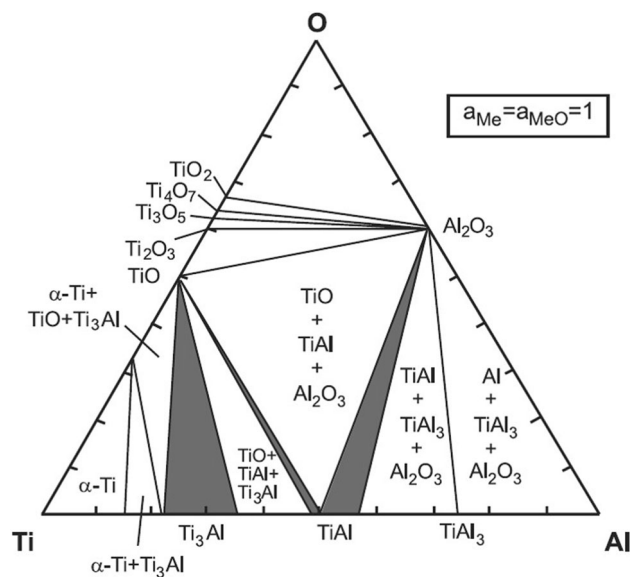

Fig. 11 Isothermal section of the Ti-Al-O phase diagram [24]

region rich in Nb. However, the presence of nitrogen has not been identified in that area (as opposed to the oxidized alloy without the deposited coating—Table 1 and 2). Due to the interdiffusion that occurs between the coating layer and the substrate of Ti-25Al-12.5Nb alloy, it is the original Al_2O_3 layer that was transformed. A small amount of Ti was found that diffused from the alloy O-Ti_2AlNb (Table 2) due the impact of high temperature. In this case, the ongoing isothermal oxidation resulted in the formation of oxide lumps
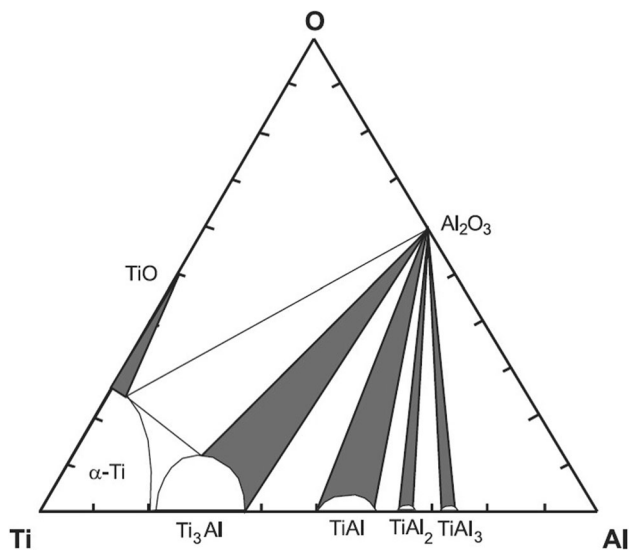
Fig. 12 Isothermal section of the Ti-Al-O phase diagram after experimental data [28]

on the surface of the sample (Fig. 7). It can be concluded that the lumps consist essentially of Al_2O_3 and TiO_2 in a lesser extent. The source of these recognizable peaks is the oxidized O-Ti_2AlNb alloy. So the oxidation of the metallic substrate of alloy-Ti_2AlNb occurred under a layer of Al_2O_3 coating. The compact and dense initial Al_2O_3 coating dissolved and in its place was taken by a porous scale. From the cross-cut metallographic specimens (Fig. 8), it can be seen that the thickness of the oxide scale is uniform. Lumps in the outer layer consist primarily of Al_2O_3. After partial wear and dissociation of the original Al_2O_3 coating, the in-core diffusion of oxygen and ex-core diffusion of Ti accelerate the scale growth.

4. Summary and Conclusions

(1) As a consequence of the isothermal oxidation in the air at the temperature of 700 °C and 800 °C, on the alloy surface of the uncoated alloy a scale forms containing mainly TiO_2, while during the oxidation of the alloy coated with Al_2O_3 an outer layer of strongly porous morphology, made of Al_2O_3, is formed.

(2) For Al_2O_3-coated alloy, forming products of oxidation showed good adhesion to the substrate, no chipping of coating/oxide layer as a result of bending loads was observed, which occurred in the case of the uncoated alloy.

(3) In the case of O-Ti_2AlNb coated with Al_2O_3, the surface coating of Al_2O_3 dissociated due to the reaction of Al_2O_3 with the O-Ti_2AlNb alloy. The reaction between Al_2O_3 and the O-Ti_2AlNb alloy is connected with the distribution of Al_2O_3, as a consequence of which the oxygen diffuses to the substrate and reacts with Ti forming oxygen compounds in the scale.

(4) On the samples of Ti-25Al-12.5 Nb, Al_2O_3 layer was stable, and these samples displayed good resistance to oxidation in set conditions and no zone of dissolved nitrogen was recorded.

Open Access

References

1. J. Kumpfert and C. Leyens, Orthorhombic Titanium Aluminides, Intermetallics with Improved Damage Tolerance, *Titanium and Titanium Alloys, Fundamentals and Applications*, C. Leyens and M. Peters, Ed., Wiley, Weinheim, 2003
2. S.A. Kakare, J.B. Toney, and P.B. Aswath, Oxidation of ductile particle reinforced Ti-48Al composite, *Metall. Mat. Trans.*, 1995, **26A**, p 1835–1845
3. K.S. Chan, Developing hydrogen-tolerant microstructures for an alpha-2 titanium aluminide alloy, *Metall. Mat. Trans.*, 1992, **23A**, p 497–507
4. A. Takasaki, Y. Furuya, and Y. Taneda, Hydrogen uptake in titanium aluminides covered with oxide layers, *Metall. Mat. Trans.*, 1998, **29A**, p 307–314
5. W. Szkliniarz, *Metallic materials with the participation of intermetallic phases (in Polish)*, Z. Bojar and W. Przetakiewicz, Ed., Technical Military Academy, Warsaw, 2006
6. S.R. Dey, S. Suwas, J.J. Fundenberger, and R.K. Ray, Evolution microstructures and textures in the orthorhombic 'O' phase due to hot rolling of the two phase (O + B_2) Ti-22Al-25Nb alloy, *Intermetallics*, 2009, **17**, p 622–633
7. J. Małecka, Investigation of the oxidation behavior of orthorhombic Ti_2AlNb alloy, *J. Mater. Eng. Perform.*, 2015, **24**, p 1834–1840
8. R. Braun and C. Leyens, Protective coatings on orthorhombic Ti_2AlNb alloys, *Mater. High Temp.*, 2005, **22**, p 437–447
9. S.G. Warrier, S. Krishnamurtby, and P.R. Smith, Oxidation protection of Ti-Aluminide orthorhombic alloys: an engineered multilayer approach, *Metal. Mater. Trans. A*, 1998, **29**, p 1279–1288
10. L. Kong, J. Qi, B. Lu, R. Yang, X. Cui, T. Li, and T. Xiong, Oxidation resistance of TiAl3-Al composite coating on orthorhombic Ti_2AlNb based alloy, *Surf. Coat. Technol.*, 2010, **204**, p 2262–2267
11. D. Arcos and M. Vallet-Regí, Sol–gel silica-based biomaterials and bone tissue regeneration, *Acta Biomat.*, 2010, **6**, p 2874–2888
12. N. Kumar et al., Effect of functional groups (methyl, phenyl) on organic-inorganic hybrid sol-gel silica coatings on surface modified SS 316, *Ceram. Internet.*, 2012, **38**, p 6565–6572
13. Z. Shi, K.G. Neoh et al., Surface functionalization of titanium with carboxymethyl chitosan and immobilized bone morphogenetic protein-2 for enhanced osseointegration, *Biomacromolecules*, 2009, **10**, p 1603–1611
14. C.J. Brinker et al., Review of sol-gel thin film formation, *J. Non Cryst. Solids.*, 1992, **147**, p 424–436
15. C.J. Brinker et al., Structure-property relationships in thin films and membranes, *J. Sol-Gel Sci. Technol.*, 1995, **4**, p 117–123
16. L.L. Hench and R. Orefice, *Sol–gel technology. Kirk-Othmer Encyclopedy of chemical technology*, Wiley, New York, 2000
17. C. Leyens and H. Gedanitz, Long-term oxidation of orthorhombic alloy Ti–22Al–25Nb in air between 650 and 800 °C, *Scr. Mater.*, 1999, **4**, p 901–906
18. C. Leyens, Environmental effects on orthorhombic alloy Ti–22Al–25Nb in air between 650 and 1000°C, *Oxid. Met.*, 1999, **52**, p 475–503
19. O. Kubaschewski and C.B. Alcock, *Metallurgical Thermochemistry*, Pergamon, New Ypor, 1983
20. G.V. Samsonov, The oxide handbook, 2nd edn. Plenum Data, New York, 1982 translated by R.K. Johnston

21. W. Mader and M. Ruhler, Electron microscopy studies of defects at diffusion-bonded Nb/Al$_2$O$_3$ interface, *Acta Mater.*, 1989, **37**, p 853–866

22. A. Rahmel, W.J. Quadakkers, and M. Schutze, Fundamentals of TiAl oxidation - a critical review, *Mater. Corros.*, 1995, **46**(271), p 271–285

23. M. Eckert, M. Hipler, Oxidation of intermetallics, (H.J. Grabke I M. Schuetze eds.), Wiley, Weinheim, 1997

24. K.L. Luthra, Stability of protective oxide films on Ti-base alloys, *Oxid. Met.*, 1991, **36**, p 274–290

25. A. Rahmel and P.J. Spencer, Thermodynamic Aspects of TiAl and TiSi$_2$ oxidation: The Al-Ti-O and Si-Ti-O phase diagrams, *Oxid. Met.*, 1990, **35**, p 53–68

26. M. Eckert, L. Bencze, D. Kath, H. Nickel, and K. Hilpert, Thermodynamic activities in the alloys of the Ti-Al system, *Int. J. Phys. Chem.*, 1996, **100**(4), p 418–424

27. N.S. Jacobson, M.P. Brady, and G.M. Mehrotra, Thermodynamics of selected Ti-Al and Ti-Al-Cr alloys, *Oxid. Met.*, 1999, **52**, p 537–556

28. M.P. Brady, B.A. Pint, P.F. Tortorelli, I.G. Wright, and R.J. Hanrahan, High temperature oxidation and corrosion of intermetallics, *Corrosion and Environmental Degradation of Materials*, M. Schütze, Ed., Wiley, Weinheim, 2000

29. G.P. Kelkar and A.H. Carim, Phase equilibria in the Ti-Al-O system at 945 °C and analysis of Ti/Al2O3 reactions, *J. Am. Ceram. Soc.*, 1995, **78**, p 572–576

30. X.L. Li, R. Hillel, F. Teyssandier, and S.J. Chou, Reactions and phase relations in the Ti-Al-O system, *Acta Metall. Mater.*, 1992, **40**, p 3149–3157

31. M. Zhang, K. Hsieh, J. Dekock, and Y.A. Chang, Phase diagram of Ti-Al-O at 1100°C, *Scr. Metall. Mater.*, 1992, **27**, p 1361–1366

32. S. Becker, A. Rahmel, M. Schorr, and M. Schütze, Mechanism of isothermal oxidation of the intermetallic TiAl and of TiAl alloys, *Oxid. Met.*, 1992, **38**, p 425–464

33. B.J. Lee and N. Saunders, Thermodynamic evaluation of the Ti-Al-O ternary system, *Zeitschrift für Metallkunde*, 1997, **88**, p 152–161

34. C. Leyens, Oxidation and Protection of Titanium Alloys and Titanium Aluminides, *Titanium and Titanium Alloys, Fundamentals and Applications*, C. Leyens and M. Peters, Ed., Wiley, Weinheim, 2003